

Detailed Comparison of the Pnicogen Bond  
with Chalcogen, Halogen, and Hydrogen Bonds

Steve Scheiner\*

Department of Chemistry and Biochemistry

Utah State University

Logan, UT 84322-0300

\*email: [steve.scheiner@usu.edu](mailto:steve.scheiner@usu.edu)

ABSTRACT

The characteristics of the pnicogen bond are explored using a variety of quantum chemical techniques. In particular, this interaction is compared with its halogen and chalcogen bond cousins, as well as with the more common H-bond. In general, these bonds are all of comparable strength. More specifically, they are strengthened by the presence of an electronegative substituent on the electron-acceptor atom, and each gains strength as one moves down the appropriate column of the periodic table, e.g. from N to P to As. These noncovalent bonds owe their stability to a mixture in nearly equal parts of electrostatic attraction and charge transfer, along with a smaller dispersion component. The charge transfer arises from the overlap between the lone pair of the electron donor and a  $\sigma^*$  antibond of the acceptor. The angular characteristics of the equilibrium geometry result primarily from a compromise between electrostatic and induction forces. Angular distortions of the H-bond are typically less energetically demanding than comparable bends of the other noncovalent bonds.

## INTRODUCTION

Noncovalent interactions have a long and storied past. They are largely responsible for the properties of condensed phases, solutions, and crystals. The forces between different segments of a large molecule fall into this category, and they guide biomolecules into their native conformations. The binding of pairs of molecules, whether gas-phase dimers, or of enzymes with their substrates, are a product of noncovalent interactions. The strengths and origins of various intermolecular forces are as varied as their applications. The extremely weak forces between rare-gas atoms in a matrix or superfluid are due primarily to dispersion/London forces that arise from instantaneous fluctuations of the electron clouds. On the other end of the spectrum are the very strong electrostatic attractions between ions of opposite charge as in the crystals of salts or ion pairs within certain proteins.

The H-bond was recognized early on as a very important type of noncovalent interaction<sup>[1-7]</sup>. It is typically formulated as the positioning of two molecules such that the H atom of one molecule, A-H, acts as a bridge to an atom D of another molecule. Usually, the A and D atoms are rather electronegative, such as O, N, or F, and the partially positively charged H atom is attracted to the lone electron pair(s) of D<sup>[8-12]</sup>. Besides the latter electrostatic attraction, there is also a certain amount of charge that is transferred from the D lone pair into a  $\sigma^*$  antibonding A-H orbital, which weakens and lengthens the A-H covalent bond, as well as shifting its stretching vibration to lower frequencies. Over the years since its earliest formulation, the H-bond has been broadened considerably<sup>[13-23]</sup>. The proton-donating and accepting atoms have generalized to less electronegative atoms, such as C, S, and Cl. And the source of electrons on the proton-acceptor molecule can be a  $\pi$ -bond, as in an alkene or conjugated system, or even a  $\sigma$ -bond. Moreover, the red shift of the A-H stretch is not universal but can occasionally reverse itself into a blue shift in certain circumstances. What remains constant however, is the bridging position of the H, and the electron transfer from proton-acceptor to donor.

Of somewhat newer vintage is another noncovalent bond in which a halogen atom, X, takes the place of the H in a bridging position<sup>[24-34]</sup>. This halogen bond has some similarities with its H-bond cousin<sup>[35,36]</sup>. Although the bridging X atom does not have a positive atomic charge, its electrostatic potential is highly anisotropic. The atom may be described as containing a ring of negative charge that surrounds a crown of positive charge along the extension of the A-X bond, sometimes referred to as a  $\sigma$ -hole<sup>[30]</sup>. It is this region which is attracted to the partial negative charge of the halogen-acceptor atom B. Like the H-bond, there is also a transfer of charge from the D atom (usually its lone pair) into the  $\sigma^*(A-X)$  orbital. Despite the switching out of the H atom for X, the halogen bond can be quite strong, competitive in many cases with a comparable H-bond. Although not as thoroughly investigated as either H or X bonds, there have been a number of indications in the literature that O or S atoms can serve a similar function in what might analogously be termed a chalcogen bond<sup>[37-51]</sup>.

### DEVELOPMENT OF THE IDEA OF A PNICOGEN BOND

Recent work in this laboratory has targeted a variation on this theme, wherein the bridging atom is a pnicogen, e.g. P. (The term pnicogen is also commonly used in the literature.) For example, the pairing of  $\text{PH}_3$  with  $\text{NH}_3$  led to an equilibrium geometry<sup>[52]</sup> which places one of the P-H bonds nearly diametrically opposite the N lone pair. This arrangement facilitates the charge transfer from the latter into the lobe of the PH  $\sigma^*$  antibonding orbital that is proximate to the P. It was noted that this pnicogen-bonding arrangement was preferable to either a  $\text{PH}\cdots\text{N}$  or  $\text{NH}\cdots\text{P}$  H-bonded configuration. Moreover, this pnicogen bond was distinct from a halogen bond in that there is no  $\sigma$ -hole in the vicinity of the P

atom. A similar pnictogen-bonded structure was found to be the global minimum also for the  $\text{PH}_3$  homodimer, wherein there is a mutual charge transfer from one P to the  $\text{PH } \sigma^*$  antibond of the other molecule, and vice versa.

Whereas the pnictogen bonds in the aforementioned hydrides are rather weak, with binding energies less than 2 kcal/mol, they can be very substantially enhanced. The replacement of the H atom in the position opposite to the lone pair of the electron donor by a more electronegative substituent<sup>[53]</sup> raises the binding energy a great deal. For example,  $\text{FPH}_2$  and  $\text{NO}_2\text{PH}_2$  each bind to a  $\text{NH}_3$  donor by more than 6 kcal/mol. In fact, this enhanced electronegativity of the substituent can yield an attraction where there is none without it. For instance, the  $\text{NH}_3$  dimer has a flat potential energy surface, containing two structures of low energy, both of which are H-bonded. However, if one of these monomers is replaced by  $\text{FNH}_2$ , a new minimum appears<sup>[54]</sup> on the surface, containing a  $\text{FN}\cdots\text{N}$  pnictogen bond, with a strength of 4 kcal/mol, competitive with the  $\text{NH}\cdots\text{N}$  H-bond in this same dimer.

It has been well understood for some time that any substituents that enhance the positive charge of the H atom on a given molecule also make the molecule a more potent proton donor in the context of a H-bond. So for example, as one, two, and three H atoms of  $\text{CH}_4$  are replaced by F, the remaining CH group is empowered to form a progressively stronger H-bond with a proton-acceptor molecule<sup>[55-57]</sup>. One might anticipate like behavior in pnictogen bonds. But surprisingly, this is not the case. When the H atoms of  $\text{FPH}_2$  were replaced by one and then two other F atoms, the  $\text{FP}\cdots\text{N}$  pnictogen bond of  $\text{FH}_2\text{P}\cdots\text{NH}_3$  did not become any stronger<sup>[58]</sup>. Indeed, there was a small weakening for each progressive substitution. This surprising behavior is not due to some anomaly of F; the same trend arises with both Cl and Br.

The strength of a pnictogen bond depends not only upon the nature of the electron acceptor but also of the donor. Calculations<sup>[59]</sup> showed that the simple hydrides followed a diminishing order of  $\text{NH}_3 > \text{OH}_2 > \text{SH}_2$ , much like is noted for H-bonds. Methyl substitution adds to it with  $\text{CH}_3\text{OH}$  stronger than  $\text{HOH}$ . Doubly-bonded O and S atoms in  $\text{H}_2\text{CO}$  and  $\text{H}_2\text{CS}$  are also improved electron donors. Like H-bonds, the pnictogen bond too can extract electron density not only from a lone pair of an electronegative atom, but also from  $\pi$ -bonds. In fact, the pnictogen bond between  $\text{FH}_2\text{P}$  and  $\pi$ -systems such as ethylene and benzene is stronger than the  $\text{OH}\cdots\pi$  H-bonds where water serves as proton donor.

The foregoing has outlined just a few similarities and differences between pnictogen and H-bonds. It would be interesting to explore these issues more thoroughly, so as to extract their root causes. The pnictogen bond has even more resemblance to halogen and chalcogen bonds, at least ostensibly. It might be tempting to lump all of these types of noncovalent bond into the same package, considering them as no more than different flavors of the same ice cream. But do they in fact represent only small variations on a theme, or do they each possess unique characteristics that differentiate them from one another? The purpose of this article is to address this fundamental question. The analysis of the various systems will take advantage of a number of windows that can only be opened via quantum chemistry, and will thus show the ability of the latter to add insight into our understanding of noncovalent bonds.

### Energetics

In some ways the most important characteristic of any noncovalent interaction is the strength with which the two entities are bound to one another. This quantity is assessed as the stabilization of the complex, relative to the two isolated subunits, all in their individually optimized geometries. This binding energy is typically evaluated in the absence of all other surrounding influences, so as to

establish a pure and unvarnished measure of the interaction. To place the following quantities in context, the H-bond energy of the water dimer in the gas phase is approximately 5 kcal/mol.

The binding energy of the pnictogen bond between the two hydrides  $\text{PH}_3$  and  $\text{NH}_3$  was calculated<sup>[52]</sup> to be 1.4 kcal/mol, and slightly weaker at 1.1 kcal/mol for the  $\text{P}\cdots\text{P}$  bond in the  $\text{PH}_3$  homodimer. These values are roughly the same<sup>[55]</sup> as the strength of a  $\text{CH}\cdots\text{O}$  H-bond in  $\text{FH}_2\text{CH}\cdots\text{OH}_2$ . However, this pnictogen bond can be strengthened very considerably by replacement of even one of the H atoms of  $\text{PH}_3$  by a more electronegative substituent<sup>[53]</sup>. A OH group, for example, increases the binding energy up to 3.6 kcal/mol, Cl up to 5.4 kcal/mol, and F to as much as 6.2 kcal/mol. It is immediately evident that even singly substituted pnictogen bonds can approach and even exceed the strengths of typical H-bonds.

How do these substituent effects on pnictogen bonds compare with the same sort of behavior of halogen and chalcogen bonds? This question was answered<sup>[60]</sup> via consideration of the Cl and S second-row neighbors of P.  $\text{PH}_3$ ,  $\text{SH}_2$ , and  $\text{ClH}$  were taken as starting points. One H atom of each molecule was replaced by substituent B, where B is one of the groups indicated on the horizontal axis of Fig 1. Each of these molecules was then paired with  $\text{NH}_3$  as the common electron donor, and the binding energy computed. For the less electronegative substituents on the left side of Fig 1, the pnictogen and chalcogen bonds are of very similar strength, both stronger than the halogen bonds. For  $\text{B}=\text{OH}$  and Cl, all three types of bonds are nearly equivalent, but the trend becomes more scattered as B becomes progressively more electronegative. The pnictogen bond is clearly the strongest for  $\text{B}=\text{NO}_2$ , and the halogen bond weakest, but this pattern completely reverses for  $\text{B}=\text{F}$  where the halogen bond energy exceeds 10 kcal/mol.

The uppermost broken curve in Fig 1 permits a comparison with the corresponding H-bonds. The binding energies of the  $\text{BH}\cdots\text{NH}_3$  complexes are almost uniformly higher than those of the other sorts of interactions. The only exception is the methyl substituent B where the  $\text{H}_3\text{CH}\cdots\text{NH}_3$  complex is bound by a bit less than are the other dimers. It is interesting to note from the far right side that FH forms a complex with  $\text{NH}_3$  that is only slightly stronger than  $\text{FCl}\cdots\text{NH}_3$ . It is also worth observing the nearly uniform increase in H-bond energy from left to right, as compared to some of the more erratic behavior of the others, BCl for instance.

Without electron-withdrawing substituents B, there is little to distinguish the H-bond energy from the pnictogen, chalcogen, and halogen bonds, as is evident from the left side of Fig 1. This point was made also in the context of the simple hydrides<sup>[61]</sup> where the binding energies of  $\text{HCl}\cdots\text{NH}_3$  and  $\text{H}_2\text{S}\cdots\text{NH}_3$  are quite similar to that in  $\text{H}_3\text{P}\cdots\text{NH}_3$ . From the perspective of the dependence of these interactions upon the particular row of the periodic table, there was little difference with  $\text{H}_3\text{As}\cdots\text{NH}_3$ . But what happens when electronegative substituents are attached - how do these interactions vary as one moves up and down in the periodic table?

In order to address this question, one can take F as a strongly electron-withdrawing substituent. The  $\text{FPH}_2$ ,  $\text{FHS}$ , and  $\text{FCl}$  molecules were paired with  $\text{NH}_3$ , as were their analogues from the first and third rows of the periodic table. Unlike the simple hydrides where there is little dependence upon electron-acceptor atom A, Fig 2 shows a fairly strong increase in the binding energy of the  $\text{FA}\cdots\text{N}$  bonds from one row of the table to the next. The pnictogen bonds are least sensitive, but even there the bond strength of 4 kcal/mol for  $\text{FN}\cdots\text{N}$  doubles in  $\text{FAs}\cdots\text{N}$ . The dependence is most dramatic for the halogen bonds, where the binding energy climbs from 2 kcal/mol for  $\text{FF}\cdots\text{N}$  all the way up to 14 kcal/mol for  $\text{FBr}\cdots\text{N}$ .

The manner in which the binding energies of the interactions in Fig 2 rise as one goes down a column of the periodic table stands in stark contrast to the behavior of H-bonds. As illustrated in Fig 2, the H-bond energy of XH with the same proton acceptor NH<sub>3</sub>, drops as one progresses from FH to ClH and then to BrH. A similar pattern has been noted previously<sup>[11,61]</sup> with H-bonds involving chalcogen and pnictogen atoms. The H-bond behaves differently even within a single row. For example, FH forms stronger H-bonds than does HOH, which is in turn a more potent proton donor than is NH<sub>3</sub>. However, the F atom results in a *weaker* halogen bond than either O or N, as may be seen in Fig. 2. In other words, when the halogen atom is itself directly involved in the bonding, viz. a halogen bond, the binding energy increases from first to second to third row. The trend is reversed in H-bonding where the halogen of XH is in a sense the “substituent” of the bridging H atom. The binding energy increases in parallel with the electronegativity of this substituent, in the order Br < Cl < F.

### Geometries

Years of investigation have led to a general picture of the factors that determine the geometry of a H-bonded complex. The AH...D structure tends toward linearity, i.e.  $\theta(\text{AH}\cdots\text{D}) \sim 180^\circ$ , and the AH bond is typically disposed along the direction of a D lone pair, if one exists. This predilection is grounded in considerations of both electrostatics and charge transfer. Another clear pattern is that stronger complexes are associated with shorter H-bonds, with the two subunits approaching one another more closely. Are these same principles transferrable to pnictogen and other bonds? Previous investigations of halogen bonds confirm these ideas there as well. The picture of the electrostatic potential around the halogen atom, described as a crown of positive charge, surrounded by a circle of negative potential, leads naturally to the linearity of halogen bonds. However, pnictogen atoms do not necessarily have such a  $\sigma$ -hole of positive charge<sup>[52]</sup>, and so the issue of their preferred orientation is not as obvious.

With regard first to the issue of intermolecular distance, it does appear that the general principle that stronger interactions are also shorter ones is valid. The R(A...D) separations diminish from left to right in Fig 3 as the B substituent becomes more electronegative, in concert with a growing interaction energy. This principle applies whether A is a pnictogen, chalcogen, or halogen. It may be noted also that the decrease is not entirely uniform. For example the length grows slightly longer in the transition from NH<sub>2</sub> to CF<sub>3</sub>, and also from Cl to NO<sub>2</sub>, for A=S and Cl, but not for P.

The lowermost broken curve in Fig 3 illustrates the parallel situation of H-bonds, where the proton donor BH consists of a proton bound to substituent B. The intermolecular distance displayed is that separating the H atom from N. These H-bond lengths are shorter than the others, primarily due to the much smaller atomic radius of H as compared to P, S, and Cl. Most importantly, the trend in the H-bond lengths is quite similar to those of the others, in particular chalcogen and halogen, in that all undergo a lengthening for B=NO<sub>2</sub>, in contrast to the more uniform lowering of R for the pnictogen bonds.

With respect to the angular aspects of the equilibrium structures, halogen bonds are simplest in that all tend toward linearity. This orientation is clearly preferred since the electrostatic alignment of the positive region of the halogen and the negative lone pair of the electron donor coincides with the maximal overlap between the latter lone pair and the pertinent lobe of the B-X  $\sigma^*$  antibonding orbital. This is not so for the chalcogen and pnictogen bonds. As in the other cases, the orbital overlap has a proclivity for linearity, but the electrostatics are a bit more subtle. It is for this reason that the BP...N angles are usually not 180°, but closer to 160-170°<sup>[53]</sup>.

An illustrative example is displayed in Fig. 4 which depicts the electrostatic potentials surrounding three molecules that engage in a pnictogen bond. The molecules chosen are  $\text{CH}_3\text{PH}_2$ ,  $\text{OHPH}_2$ , and  $\text{FPH}_2$  which cover a wide range of strength of the interaction. The blue regions indicate positive potential, and negative regions are designated by red. The red arrow pointing directly to the right represents the extension of the B-P covalent bond, along which the electron donor molecule could best align its lone pair with the B-P  $\sigma^*$  antibond. The green arrow, on the other hand, indicates the optimal alignment if the only consideration were electrostatics, pointing along the most positive region of the potential. The black arrows, designating the actual angle at which the N atom actually lies in the equilibrium geometry of each complex with  $\text{NH}_3$ , is thus the result of a compromise between these two factors, and is hence situated between the red and green arrows.

Having established the principles guiding the establishment of the equilibrium configuration of the various sorts of noncovalent bonds, it would be valuable to have some information about the strength of the tendency toward this relative orientation. That is, how difficult is it to make a H-bond nonlinear, or to bend the pnictogen bond away from its favored structure? This problem can be addressed in a straightforward manner by quantum chemical methods. Starting with the equilibrium geometry of each dimer, the distance between the two subunits was held constant, but the orientational angle of each was incremented by fixed amounts<sup>[62]</sup>. Optimization of the remainder of the structure traced out a curve that had a very nearly parabolic shape,  $E = \frac{1}{2} k(\Delta\theta)^2$ . The force constant  $k$  provides a simple measure of the resistance of each complex to angular distortion. These force constants are reported in the first column of data in Table 1. For each type of bond, pnictogen, chalcogen, or halogen, the three substituents  $B = \text{F}$ ,  $\text{Cl}$ , and  $\text{CF}_3$  are added to encompass a range of interaction energies. The last four rows of Table 1 contain related data for various H-bonded systems for purposes of comparison.

Comparison of the data indicates little distinction between the stiffness of the pnictogen, chalcogen, and halogen bonds for substituent  $\text{F}$ . However, the pnictogen bond is more resistant to distortion than are the other sorts of bonds for the remaining substituents. In most cases,  $k$  is smallest for the H-bonds. It is commonly anticipated that the stiffness of any bending motion will be related to the strength of the bond being bent. The binding energy  $\text{BE}$  is reported in the next column of Table 1, followed in the last column by the ratio  $(k/\text{BE})$ . This latter quantity might be considered the best measure of true stiffness as it considers both prime factors. Comparison of the data in the last column first shows that H-bonds are much easier to bend than are the others, with  $k/\Delta E$  ratios between 1.6 and 2.8, smaller than the values observed for any of the other systems. Within the latter set, the pnictogen bonds appear to be stiffer than either chalcogen or halogen bonds, which are comparable to one another.

Due to the transfer of electron density into a H-A  $\sigma^*$  antibonding orbital, the A-H bond of a  $\text{AH}\cdots\text{D}$  H-bond usually weakens and elongates. One can expect a similar lengthening in the B-A bonds of pnictogen and other bonds. The changes in the relevant bond lengths are listed in Table 2 for the various sorts of noncovalent bonds. In most cases there is in fact a progressive lengthening as the substituent  $B$  becomes more electronegative and the intermolecular interaction strengthens. However, the trends are not uniform by any means. For one thing, there are a few small contractions in the bond, particularly for the weaker interactions. And the  $B=\text{Cl}$  substituent is associated with a particularly large bond elongation, perhaps because  $\text{Cl}$  lies in the second row of the periodic table. There are some particular irregularities with the  $\text{NO}_2$  substituent, which is especially variable depending on the nature of the  $A$  atom, even to the point of suffering a large  $\text{Cl-N}$  bond contraction in the  $\text{NO}_2\text{Cl}\cdots\text{NH}_3$  halogen-bonded

complex. In summary, the bond length changes in Table 2 do not provide any general rules to distinguish H-bonds from pnictogen, chalcogen, or halogen bonds.

### Electron Density Shifts

With the use of the NBO procedure, it is possible to quantify the amount of charge that is being transferred from the electron-donor lone pair to the relevant  $\sigma^*$  antibonding orbital of the electron acceptor. The energetic consequence of this transfer is defined as a second-order perturbation energy  $E(2)$ , and these values are listed in Table 3, for the same systems described in Table 2. There are some clear correlations between the quantities in these two tables, which is sensible since it is the charge transfer that is largely responsible for the elongation of the covalent bonds. In either case, there is a tendency for the quantities to enlarge as the bond becomes stronger as one progresses from top to bottom in either table.

One might also note that the charge transfer energies tend to be greater for the H-bonds in the last column than for the other sorts of noncovalent bonds. Yet this distinction does not translate into consistently larger bond elongations for the H-bonds. With respect to either  $\Delta r$  in Table 2, or  $E(2)$  in Table 3, there is no clear pattern that distinguishes the pnictogen from the chalcogen and halogen bonds. There are other signs that the two properties are not precisely correlated. For example, the A-NO<sub>2</sub> bonds are shortened for A=S and Cl even though some charge goes into the  $\sigma^*(A-N)$  antibond.

Of course the charge transfers in Table 3 represent only one small segment of all of the electron density rearrangement that accompanies formation of a pnictogen bond or any other complex for that matter. One can achieve a more thorough outlook by examining electron density redistribution maps. Fig 5 displays the increases (purple) and decreases (yellow) of total electron density that result from the formation of the complex from the individual isolated monomers. As reflections of total density, these maps are not limited to any individual MO, localized as in NBO or otherwise. A second advantage is that one can observe changes occurring in all of space, not just in the vicinity of the intermolecular charge transfer. These maps also provide information on charge shifts occurring within each monomer, polarizations resulting from the electric field of its partner in the dimer.

The four complexes displayed in Fig 5 represent the combinations of FH<sub>2</sub>P, FHS, FCl, and FH with common electron donor NH<sub>3</sub>. The use of the fluorosubstituent in all systems permits a degree of uniformity so as to facilitate a comparison. A cursory examination of the four maps in Fig 5 reveals a number of features that are common among pnictogen, chalcogen, halogen, and H-bonded systems. Focusing first on the intermolecular region between the A and N atoms, there is a yellow region of density loss to the right of A, then a smaller purple gain, and finally another loss to the immediate left of N. As one proceeds from P to S to Cl, these regions become progressively smaller, indicating lesser degrees of charge shift. In the case of the H-bonded system of Fig 5d, the first yellow region surrounds the bridging proton, a distinction from the other complexes.

Turning next to the peripheral regions, outside of the A...N interaction region, there is a large yellow region of charge loss to the right of each NH<sub>3</sub> molecule, indicating it is this area which is the ultimate source of the charge being transferred across to the electron acceptor molecule. This region becomes larger from P to S to Cl, which is consistent with the growing transfer from the NH<sub>3</sub> molecule reported in the last row of Table 2. On the left side of the A atoms, there is a pattern of purple charge gain on both sides of the F atom. Again, this set of contours encompasses a larger area from Fig 5a to 5c, also consistent with the idea of enhanced intermolecular charge transfer in this order. In summary, the

patterns of charge shift indicate only small shades of difference between the pnictogen, chalcogen, and halogen bonds, more a matter of degree than of anything fundamentally different. The same consistency applies to the H-bond in Fig 5d.

As just noted, the lone pair region of the N atom in Fig 5 shows what appears to be a gain of electron density upon formation of the complex in all four systems. Does this observation contradict the idea of charge transfer out of this lone pair as a primary stabilizing factor for these bonds? In order to answer this question, one must recall that the latter  $n \rightarrow \sigma^*$  transfer is associated only with a single pair of orbitals, whereas the total density shifts in Fig 5 arise from consideration of all orbitals cumulatively. In other words, while density may be extracted from the lone pair in question, a larger amount shifting *into* this region from the outer regions of the  $\text{NH}_3$  molecule would easily explain the total increase observed in Fig. 5.

And indeed, very recent work reinforces this idea. Mo et al <sup>[63]</sup> considered the  $\text{OH} \cdots \text{O}$  H-bonds formed between formic acid molecules, and divided the electron redistributions that occur upon formation of the dimer into two separate contributions. The shifts that are attributed to the transfer of total density from one monomer to the other clearly show the loss of density from the lone pair of the proton-acceptor atom, and the gain in the  $\sigma^*$  region of the covalent O-H bond of the proton donor, verifying the predictions of a score of NBO analyses of numerous H-bonds. On the other hand, the pattern that results directly from polarization effects, i.e. redistributions within each monomer, caused by the presence of the partner molecule's electric field, is just the opposite, but larger in magnitude. In other words, the loss of density in the proton acceptor lone pair due to a very real  $n \rightarrow \sigma^*$  charge transfer is masked by a larger density increase in this same region associated with intramolecular rearrangements. The combination of these two effects into a single map of charge density shift thus shows the familiar increase of density in the lone pair area.

It is stressed that the polarization-induced shift in no way diminishes the importance, nor the energetic consequence, of the contribution of the intermolecular  $n \rightarrow \sigma^*$  charge shift to the stability of these bonds. There are no other intermolecular orbital-to-orbital charge transfers that are comparable in magnitude to this particular shift. The primary nature of this particular charge shift, as compared to any others, is verified by another observation. The changes in orbital populations of the N lone pair and the A-H  $\sigma^*$  orbitals are the largest of any NBO orbital in either molecule, in any system considered.

#### Energy Decomposition

One unique strength of quantum chemical methods is the capability to dissect an interaction into its component parts. Of course, there is no one correct way to carry out this process, and a number of different philosophies have been developed over the years. The early Kitaura-Morokuma (KM) procedure <sup>[64,65]</sup> broke the total into first and higher-order terms. The former was further partitioned into two pieces. The electrostatic (ES) term represented the purely electrostatic interaction between the charge distributions of the two monomers, prior to allowing the density of either subunit from being affected by the other. The exchange (EX) component is comparable to the classic steric repulsion, representing the Pauli exchange between the electron clouds of the two subunits. Once the two monomers are permitted to perturb one another, the resulting second-order perturbation contains first a polarization energy (POL) which represents the stabilization arising from any shifts of charge contained wholly within one molecule or the other. The charge transfer component is similar, but is associated with shifts of charge from A to D and vice versa. The KM scheme did not include all components, so

there remained a so-called MIX term from higher-order effects. Nor did it include electron correlation so ignored any contributions from dispersion energy.

Ongoing theoretical advances<sup>[66,67]</sup> resulted in the development of symmetry-adapted perturbation theory (SAPT) to the point where it could be routinely applied to intermolecular interactions. This procedure also yields electrostatic and exchange energies, but at more than one level of perturbation. Rather than separating the effects of mutual perturbation into internal polarization and external charge transfer, SAPT combines the total under the rubric of induction energy (IND). And the nature of SAPT permits a direct evaluation of dispersion energy (DISP), an advantage over KM theory. The effects of exchange are considered upon each of these quantities, so SAPT formulation includes such terms as exchange-induction and exchange-dispersion as separate quantities.

The benefits of SAPT energy decomposition can be applied to help understand the similarities and differences of the pnictogen and other bonds. As in the previous cases, the fluorosubstituted  $\text{FH}_2\text{P}$ ,  $\text{FHS}$ ,  $\text{FCl}$ , and  $\text{FH}$  were each allowed to form a complex with  $\text{NH}_3$  as universal electron donor. The breakdown of the total interaction energy into its component parts is reported in Table 4 for these dimers. Reading from left to right, one can see a growth in all components as one progresses from pnictogen to chalcogen to halogen bond. For example, the electrostatic attraction in  $\text{FH}_2\text{P}\cdots\text{NH}_3$  of  $-18.2$  kcal/mol doubles to  $-35.9$  kcal/mol in  $\text{FCl}\cdots\text{NH}_3$ . There is an even more dramatic rise in induction energy, more than threefold. The repulsive exchange energy also climbs sharply, counteracting the increases of the attractive components, which lessens the growth of the total interaction energy from  $7.2$  kcal/mol in the pnictogen bond to  $10.4$  kcal/mol for  $\text{FCl}\cdots\text{NH}_3$ . In terms of the relative contributions of each term, ES and IND are very nearly equal for  $\text{FH}_2\text{P}\cdots\text{NH}_3$  but the latter is twice as large as the former in the halogen bond. While dispersion energy is significant for all systems, it is consistently the smallest component.

Turning finally to the H-bond in the last column of Table 4, the electrostatic attraction is intermediate between the two extremes of  $\text{FH}_2\text{P}$  and  $\text{FCl}$ , close to the value for the chalcogen bond. Induction energy in the H-bond is small, and the dispersion is also the smallest of all the complexes in the table. So one feature that is distinct for the H-bond is the ratio of IND to ES. Whereas the former is at least as large as, or bigger than ES for the other systems, IND is roughly half the magnitude of ES for the H-bond. Likewise, the dispersion energy accounts for a smaller fraction of the total for  $\text{FH}\cdots\text{NH}_3$  than for the other complexes. One may note finally that the exchange repulsion for the H-bond is disproportionately small, and this fact contributes to the large binding energy in  $\text{FH}\cdots\text{NH}_3$ . The low exchange repulsion, despite the close approach of the two molecules in the H-bonded complexes (see Fig 3), is likely due to the small atomic radius of the bridging H atom.

As indicated above, the manner of partitioning the total interaction energy is an arbitrary one, so there is no unique and “correct” means of doing so. It is important then to compare the conclusions arising from one scheme, SAPT for example, with another. Such a comparison with the Kitaura-Morokuma (KM) prescription was carried out for the pnictogen bond in  $\text{H}_3\text{P}\cdots\text{NH}_3$ <sup>[52]</sup> and revealed basic similarities. The first-order terms, electrostatic attraction and exchange repulsion were nearly identical from one scheme to the other. The KM polarization and charge transfer energies, which can be considered roughly as the two prime components of induction energy, summed to a total that was within 17% of the SAPT induction energy. This reasonable coincidence of values adds to the confidence which one can place in the SAPT technique.

## Level of Theory

Given the broad diversity of different quantum chemical methods that have been applied to various systems over the years, it is important to consider which are most appropriate to study these noncovalent bonds. In the first place, dispersion is an important component of all of these interactions, even if not the primary one. As many of the variants of DFT either ignore dispersion entirely, or attack it in an approximate manner, one would not anticipate DFT methods to be reliable. There are new procedures and DFT functionals under current development which show promise in this regard, but their accuracy has not undergone thorough testing as yet to be considered reliable.

In terms of inclusion of electron correlation, CCSD(T) is sometimes considered a “gold standard” in treating molecular interactions, particularly when used in conjunction with a sufficiently large and flexible basis set. While the computational expense of CCSD(T) may perhaps keep it from being the daily method of choice, it is possible in many cases to carry out some benchmark calculations by which to assess the reliability of methods such as MP2, which is considerably more economical.

Such a test was carried out on a set of pnictogen bonds of varying strength. The  $\text{BH}_2\text{P}\cdots\text{NH}_3$  complexes were evaluated for the full range of B, from weak  $\text{CH}_3$  to strong F<sup>[53]</sup>. All geometries were optimized at the MP2/aug-cc-pVDZ level, and binding energies all corrected by the counterpoise procedure<sup>[68]</sup>. At the MP2 level, the increase in size and flexibility of the basis set in going from aug-cc-pVDZ to aug-cc-pVTZ produces a small increase in the binding energy. Upgrading the treatment of electron correlation from MP2 to CCSD(T), again with the larger set, lowers the binding energy, but by a fairly small amount. As a result, MP2/aug-cc-pVDZ calculations would appear to offer a reasonably accurate, although a slight underestimate of the binding energies of all eight of these pnictogen bonds.

While both the aug-cc-pVDZ and aug-cc-pVTZ basis sets are reasonably flexible, the question remains as to what would be the effect of enlarging further. There are a number of prescriptions that have been developed which permit an ordered and systematic asymptotic approach to a complete basis set. One of these procedures was tested, again in the context of these same pnictogen bonds. The method selected<sup>[69]</sup> extrapolates both the SCF and correlation energies separately, and is designed to use VDZ and VTZ basis sets as its input data.

The procedure was tested on the same set of pnictogen-bonded complexes pairing  $\text{BH}_2\text{P}$  with  $\text{NH}_3$ . This scheme was found to be quite well suited to these noncovalent interactions, extrapolating smoothly to an infinite-size basis set. All levels of theory, with either basis set, with and without extrapolation, and with or without counterpoise correction, provide a similar ordering of the binding energy with respect to the substituent B. Not unexpectedly, SCF values are much too small, but MP2 data are similar to CCSD(T) quantities. Even when extrapolated, it remains necessary to include counterpoise corrections to the basis set superposition error. On a statistical basis, if the full extrapolation to the CCSD(T) result is not feasible, the best option appears to be extrapolation of (counterpoise-corrected) MP2 data, the mean absolute error of which is 0.25 kcal/mol. Almost as accurate is the unextrapolated MP2/aug-cc-pVTZ level, with an error of 0.27 kcal/mol. Testing of this procedure on the water dimer provided an optimistic assessment that this scheme ought to be useful for H-bonds as well.

## Other Calculations

The intriguing properties of pnictogen bonds have motivated interest by a number of other theoretical groups. A very early study<sup>[70]</sup> of the  $\text{PH}_3$  dimer suggested a single minimum on its surface, whose geometry appeared to suggest a pair of bifurcated  $\text{PH}\cdots\text{P}$  H-bonds rather than a pnictogen-bonding

arrangement. But the optimization included no correlation, so the structure is suspect, as was that of the later  $\text{NH}_3/\text{PH}_3$  heterodimer<sup>[71]</sup> which contained H-bonds, albeit weak ones. Later optimizations of the  $\text{PH}_3$  dimer on a correlated surface<sup>[72,73]</sup> identified a linear  $\text{HP}\cdots\text{PH}$  arrangement as the global minimum, bound by 1.4-1.6 kcal/mol, in which a  $\text{P}_{\text{lp}}\rightarrow\sigma^*(\text{PH})$  charge transfer was suggested<sup>[72]</sup> as a potential source of stability. This geometrical arrangement was noted to be the global minimum for a range of substituted  $\text{X}_3\text{E}\cdots\text{EX}_3$  interactions<sup>[74,75]</sup> wherein E represents any general pnictogen, and X one of several halogens.

The addition of a range of different substituents on the two P atoms was reported<sup>[76]</sup> to produce a rather strong effect upon the binding energy, in conformity with our own findings. This idea was reinforced in symmetric systems<sup>[77]</sup> which were associated with binding energies as large as 8 kcal/mol, consistent with our data. This latter study also noted that the one-bond spin-spin coupling constants exhibited a quadratic dependence upon the  $\text{R}(\text{P}\cdots\text{P})$  distance. Calculations of intramolecular  $\text{P}\cdots\text{P}$  interactions<sup>[49]</sup> confirmed the concept of  $\text{P}_{\text{lp}}\rightarrow\sigma^*\text{PX}$  charge transfer as a strong stabilizing influence. Consistent with our findings that multiple halogens on a single pnictogen center can be counterproductive, it was later noted<sup>[78]</sup> that F substituents that are not actively involved in the charge transfer tend to weaken the  $\text{P}\cdots\text{P}$  pnictogen bond.

In addition to our own examination of the combined effects of multiple pnictogen and H-bonds<sup>[79]</sup>, other work has also considered the issue of cooperativity. The general conclusion<sup>[80-83]</sup> reinforces the venerable idea that these bonds; pnictogen, hydrogen, halogen, etc., mutually strengthen one another, i.e. positive cooperativity, when the central molecule acts as simultaneous electron donor and acceptor. Our contention that  $\pi$  bonds can act as a source of electron density in a pnictogen bond has also been affirmed<sup>[84]</sup>.

There has been some contention as to the origin of the stability of pnictogen bonds. Politzer and coworkers<sup>[46,85,86]</sup> have made a case that electrostatics is the primary factor, which is based primarily on the correlation they have observed between the total binding energy on one hand, and the maximum positive electrostatic potential on a chosen surface that encloses the pnictogen-containing monomer on the other. And indeed, such a correlation has been confirmed by our own calculations in which the electrostatic energy is computed directly. On the other hand, there is also a strong correlation between binding energy and other factors, such as induction and dispersion<sup>[87]</sup>, so one should be reluctant to assume any of these components are the sole contributing factor. As a second point, it is not only electrostatics but also induction, especially the  $\text{lp}\rightarrow\sigma^*$  charge transfer, that is highly anisotropic and contribute to the preferred angular orientation of the two monomers in each complex, as described above. The substantial contributions of induction have been verified by other workers<sup>[88]</sup>. There have been other works that suggested a more important role for dispersion as well<sup>[75,89,90]</sup>.

With regard to the necessary level of theory, Wang et al noted<sup>[72]</sup> quite low sensitivity of the binding energy of the  $\text{PH}_3$  dimer to basis set, varying from 6-311G(3d,3p) up to 6-311++G(3df,3pd). Enlargement of basis set from aug-cc-pVTZ to aug-cc-pVQZ was found to have only a small effect on LCCSD(T) binding energies of halogenated  $\text{X}_3\text{E}\cdots\text{EX}_3$  dimers<sup>[75]</sup>, as was observed in our own studies described above.

### Experimental Observations

Experimental verification of these sorts of noncovalent bonds arises primarily from analysis of crystal structures. These systems are distinct from the gas phase studied by the theoretical calculations

in that any such bonds are part of larger molecules, and further that they are surrounded by other molecules as well. Considering P...N pnictogen bonds first, when PBr<sub>3</sub> was paired with 1,4-dimethylpiperazine, the two molecules were oriented<sup>[91]</sup> such that one of the Br atoms of PBr<sub>3</sub> lies directly opposite the N atom, with a  $\theta(\text{BrP}\cdots\text{N})$  angle of 179.5°, and the N lone pair points directly toward the P atom. The intermolecular R(P...N) distance is 2.802 Å, very close to distances computed<sup>[58]</sup> for trihalogenated systems. Computations of the complex of PBr<sub>3</sub> with N(CH<sub>3</sub>)<sub>3</sub> found<sup>[58]</sup> a BrP...N angle within 5° of linearity, and this P-Br bond was longer than the other two P-Br bonds by 0.08 Å, in perfect agreement with the experimental observations. A later work<sup>[92]</sup> likewise identified a P...N noncovalent interaction in the structure of a hypercoordinate acetylene phosphorus molecule. One P-bonded acetylenic group lies directly opposite the N atom,  $\theta(\text{CP}\cdots\text{N})=177^\circ$ , whose P-C bond length is longer by 13.4 mÅ than the other P-C bond. Short P...N distances (2.44-2.57 Å) were also identified<sup>[93]</sup> in an intramolecular contact involving three separate molecules, wherein P was covalently bonded to 2 Cl atoms, and N bonded to three methyl groups. In all cases, the alignment was nearly linear, with  $\theta(\text{ClP}\cdots\text{N})=172\text{-}174^\circ$  and once again, there was a significant stretch, by 0.08 Å, of the P-Cl bond that lay opposite the N atom.

In terms of a pnictogen bond involving a pair of P atoms, structure determination<sup>[94]</sup> of a series of disphospha-functionalised naphthalenes found R(P...P) distances of 2.77-2.81 Å. The structure of 1,2-(diphenylphosphino)-1,2-dicarba-*closo*-dodecaborane<sup>[95]</sup> and related molecules<sup>[96]</sup> contained interphosphorous distances in the range between 3.15 and 3.22 Å, attributed to electron donation from the lone pair of one P to the antibonding P-C orbital of the other. P...P distances of 3.318 Å were observed<sup>[97]</sup> in the X-ray structure of (C<sub>6</sub>F<sub>5</sub>)<sub>2</sub>PCH<sub>2</sub>P(C<sub>6</sub>F<sub>5</sub>)<sub>2</sub>. P...P bonding, with R=2.78 Å, occurs also in in *p*-C<sub>6</sub>H<sub>4</sub>[N(PCl<sub>2</sub>)<sub>2</sub>]<sub>2</sub> where it leads to the formation of a two-dimensional sheetlike structure<sup>[74]</sup>. More recent work found short P...P distances in a series of *closo*-dicarbaboranes<sup>[98]</sup> and in peri-1,8-disubstituted naphthalenes<sup>[49]</sup>. In both cases, calculations confirmed P<sub>lp</sub>→σ\*(P-X) charge transfer as a contributing factor.

Turning to the N...N pnictogen bond, an early study<sup>[99]</sup> of (N,N-difluoroamino)-2,4,6-trinitrobenzene found an internitrogen separation of 3.06 Å wherein the N-C bonds were arranged in a manner consistent with N<sub>lp</sub>→σ\*(NC) donation. The two N atoms of a N-(difluoroamino)azole<sup>[100]</sup> are separated by 3.12 Å. The F atom is disposed 165° from the N...N axis, precisely the same angle as predicted by calculations<sup>[54]</sup>. A study of bis(difluoramino)-substituted nitrogen heterocycles<sup>[101]</sup> yielded FN...N configurations with R(N...N)= 2.99 and 2.79 Å, with  $\theta(\text{FN}\cdots\text{N})$  angles of 149° in two different molecules. A later analysis of the crystal structure of a molecule containing gem-difluoroamino groups<sup>[102]</sup> placed the two N atoms 3.02 Å apart, and an F atom lies 150° from the N...N axis. In the case of chlorosubstitution, a 1992 study of a pendent-arm macrocycle dichloroamine<sup>[103]</sup> found two N atoms separated by 2.84 Å, and the  $\theta(\text{ClN}\cdots\text{N})$  angle is 161°, again quite close to the computational prediction. The possibility that π orbitals can serve as a source of charge in a pnictogen bond was confirmed<sup>[89]</sup>, at least for the heavier pnictogens of As, Sb, and Bi, via analysis of crystal structures.

The literature contains some confirmation of the stability of complexes of the BS...N type as well. Surveys of crystal structures prior to 1980<sup>[37]</sup>, for example, noted a propensity for nucleophiles to approach a divalent S atom approximately along an extension of a S-X bond, a tendency confirmed<sup>[42]</sup> later. What appears to be a N...S bond was observed<sup>[104]</sup> within N-acetylglycine ethyl dithioester with N and S separated by only 2.89 Å, and a  $\theta(\text{CS}\cdots\text{N})$  angle of 161°. The pnictogen bond between two As

atoms, with  $R(\text{As}\cdots\text{As}) = 2.37 \text{ \AA}$  has been observed in the crystal <sup>[105]</sup> of cyclopentadienyl- $\text{AsX}_2$ . And finally, crystal diffraction studies <sup>[106]</sup> also support the idea of the charge transfer to a  $\pi^*$  orbital that calculations imply is a contributing factor to the stability of the pnictogen bonds involving unsaturated systems.

## CONCLUSIONS AND PERSPECTIVES

The application of quantum chemical techniques has brought into view a number of similarities and differences between the pnictogen bond on one hand, and halogen, chalcogen, and H-bonds on the other. All depend on a confluence of electrostatic, induction, and dispersion forces. The bridging proton in a H-bond is positively charged, so its attraction to the partial negative charge of the proton-acceptor atom of the partner subunit is straightforward. A bridging halogen atom contains a limited region of positive charge, directed along an extension of the B-X bond, which serves the same purpose. Electrostatic forces play an important role in pnictogen bonds as well, even in the absence of a pure crown of positive charge. Elucidation of the electrostatic potential around the periphery of the electron acceptor molecule shows how its interaction with that of the donor helps guide the two molecules into their equilibrium structure.

A second important component of all of these noncovalent bonds rests upon the charge transfer that takes place from the donor molecule (usually, but not always, its lone pair) into a  $\sigma^*$  antibonding orbital of the acceptor. This phenomenon is aided by a linear alignment of the  $\text{BA}\cdots\text{D}$  atoms, which can be perturbed to a certain limited extent by electrostatic considerations that arise in the case of the pnictogen and chalcogen bonds. The additional charge in the antibonding orbital typically leads to an elongation of the relevant B-A covalent bond in the complex, although such bond length changes are not as regular as some of the other facets of these noncovalent bonds.

There is a growth in the electrostatic and inductive attractive components as one progresses from pnictogen to chalcogen to halogen bond, but a like increase in exchange repulsion leads to a fairly steady set of total interaction energies. ES and IND are roughly equal in the pnictogen bonds but the latter is twice as large as the former in the halogen bond. The H-bond contains a proportionately larger contribution from electrostatic energy, and a smaller contribution from exchange repulsion. While dispersion energy is significant for all systems, it is consistently the smallest component.

All bonds are strengthened when an electronegative substituent B is added to the electron acceptor molecule, although there are some irregularities from one type of bond to the next. H-bonds tend to be stronger than the others for a given substituent. As the A atom is drawn from a lower row of the periodic table, as in the progression from N to P to As, the pnictogen bond gains strength, as do the chalcogen and halogen bonds. The latter is particularly sensitive to such atom substitutions as the  $\text{FBr}\cdots\text{NH}_3$  bond is an order of magnitude stronger than the analogue where the Br is replaced by F. The behavior of the H-bonds is directly opposite; the lowering of the row in the periodic table diminishes, rather than enhances, each H-bond. In the absence of an electronegative substituent, as in the simple hydrides, the strength of these interactions is fairly similar from one bond to the next, and is likewise insensitive to the row of the periodic table in which the A atom lies. In an unusual observation, the presence of more than one electron-withdrawing substituents on the A atom has a progressive strengthening effect on the H-bond, but no such perturbation on the pnictogen bond.

In all the interactions discussed here, stronger bonds are associated with shorter intermolecular separations. The  $R(\text{H}\cdots\text{D})$  distance is shorter in H-bonds than in the others, due in large measure to the

smaller atomic radius of H. All the interactions tend toward linearity, although the pnicogen and chalcogen bonds are somewhat distorted due to the aforementioned electrostatic considerations. The H-bond is most easily distorted from its optimal orientation, which can be ascribed to the smaller size of H, which lessens the steric repulsions for distorted geometries.

There are similarities amongst all interactions with respect to shifts of electron density. The charge transfer from the lone pair of the electron donor atom is compensated by internal shifts that result in a net increase in total density in this region. There is a net loss in the region to the immediate right of the A atom, which accounts for the more positive charge of the bridging proton upon formation of a H-bond.

The identification of all the minima on each potential energy surface <sup>[52,54,59-61,107,108]</sup> has provided a wealth of additional information concerning comparative strengths of different sorts of interactions. Some general rules that may be extracted are as follows. When a halogen X is added to an NH group it of course strengthens it as a proton donor, making a XNH...N H-bond the strongest interaction for XNH<sub>2</sub>. In the case of X=F, the FN...N pnicogen bond is the secondary interaction, while halogen bonds NX...N are secondary for X=Cl, Br. Adding a halogen to SH produces different preferences for each X. When X=F or Cl, the XS...N chalcogen bond predominates, but a BrSH...N H-bond is preferred for Br, with a BrS...N chalcogen bond secondary. Halogen bonds of the SX...N type are weaker. The OH group is a powerful proton donor so XOH...N H-bonds are the preferred structure, stronger than a halogen bond.

Although perhaps still sporadic, there have been strong indications of the presence of pnicogen bonds drawn from diffraction studies of crystals. It is hoped that some of the concepts enunciated here may encourage workers in that area to analyze the structures arising from their measurements for more such examples, or to perhaps target their research toward systems where such bonds are considered likely. The work related here provides evidence that pnicogen bonds can be quite strong, so that their observation in gas phase dimers ought to be feasible, given judiciously chosen systems. Indeed, calculations have indicated that pnicogen bonds might be observed in clusters larger than dimers in the gas phase <sup>[79]</sup>.

In summary, pnicogen bonds would appear to represent a very real type of noncovalent interaction, with certain parallels to chalcogen and halogen bonds, as well as H-bonds. It is certainly conceivable that ideas about the forces that control their strength will ultimately be applied to the design of large molecular systems that incorporate pnicogen bonds into the structure, in the same way that H and halogen bonds are used in crystal engineering.

## REFERENCES

- [1] C. M. Huggins, G. C. Pimentel, J. N. Shoolery, *J. Chem. Phys.*, **1955**, *23*, 1244.
- [2] G. C. Pimentel, A. L. McClellan *The Hydrogen Bond*; Freeman: San Francisco, 1960.
- [3] P. A. Kollman, L. C. Allen, *Chem. Rev.*, **1972**, *72*, 283.
- [4] M. D. Joesten, L. J. Schaad *Hydrogen Bonding*; Marcel Dekker: New York, 1974.
- [5] *The Hydrogen Bond. Recent Developments in Theory and Experiments*; P. Schuster, G. Zundel, C. Sandorfy, Eds.; North-Holland Publishing Co.: Amsterdam, 1976.
- [6] R. Taylor, O. Kennard, W. Versichel, *J. Am. Chem. Soc.*, **1983**, *105*, 5761.
- [7] P. Schuster *Hydrogen Bonds*; Springer-Verlag: Berlin, 1984; Vol. 120.
- [8] G. A. Jeffrey, W. Saenger *Hydrogen Bonding in Biological Structures*; Springer-Verlag: Berlin, 1991.
- [9] S. Scheiner. Ab initio studies of hydrogen bonding. In *Theoretical Models of Chemical Bonding*; Maksic, Z. B., Ed.; Springer-Verlag: Berlin, 1991; Vol. 4; pp 171.
- [10] *Theoretical Treatments of Hydrogen Bonding*; D. Hadzi, Ed.; John Wiley & Sons: Chichester, 1997, pp 297.
- [11] S. Scheiner *Hydrogen Bonding. A Theoretical Perspective*; Oxford University Press: New York, 1997.
- [12] G. Gilli, P. Gilli *The Nature of the Hydrogen Bond*; Oxford University Press: Oxford, UK, 2009.
- [13] M. Nishio, Y. Umezawa, K. Honda, S. Tsuboyama, H. Suezawa, *CrystEngComm*, **2009**, *11*, 1757.
- [14] I. Alkorta, J. Elguero, J. E. D. Bene, *Chem. Phys. Lett.*, **2010**, *489*, 159.
- [15] B. J. v. d. Veken, S. N. Delanoye, B. Michielsen, W. A. Herrebout, *J. Mol. Struct.*, **2010**, *976*, 97.
- [16] S. Scheiner, Y. Gu, T. Kar, *J. Mol. Struct. (Theochem)*, **2000**, *500*, 441.
- [17] A. Karpfen, E. S. Kryachko, *Chem. Phys. Lett.*, **2010**, *489*, 39.
- [18] M. Domagala, S. J. Grabowski, *Chem. Phys.*, **2010**, *367*, 1.
- [19] S. Scheiner, T. Kar, Y. Gu, *J. Biol. Chem.*, **2001**, *276*, 9832.
- [20] E. Arunan, G. R. Desiraju, R. A. Klein, J. Sadlej, S. Scheiner, I. Alkorta, D. C. Clary, R. H. Crabtree, J. J. Dannenberg, P. Hobza, H. G. Kjaergaard, A. C. Legon, B. Mennucci, D. J. Nesbitt, *Pure Appl. Chem.*, **2011**, *83*, 1637.
- [21] H. S. Biswal, E. Gloaguen, Y. Loquais, B. Tardivel, M. Mons, *J. Phys. Chem. Lett.*, **2012**, *3*, 755.
- [22] S. Scheiner, S. J. Grabowski, T. Kar, *J. Phys. Chem. A*, **2001**, *105*, 10607.
- [23] M. Solimannejad, M. Gharabaghi, I. Alkorta, G. Sánchez-Sanz, *Struct. Chem.*, **2012**, *23*, 847.
- [24] K. E. Riley, P. Hobza, *J. Chem. Theory Comput.*, **2008**, *4*, 232.
- [25] I. Alkorta, F. Blanco, M. Solimannejad, J. Elguero, *J. Phys. Chem. A*, **2008**, *112*, 10856.
- [26] A. Karpfen. Theoretical characterization of the trends in halogen bonding. In *Halogen Bonding. Fundamentals and Applications*; Metrangolo, P., Resnati, G., Eds.; Springer: Berlin, 2008; Vol. 126; pp 1.
- [27] D. Hauchecorne, R. Szostak, W. A. Herrebout, B. J. v. d. Veken, *ChemPhysChem.*, **2009**, *10*, 2105.
- [28] M. G. Sarwar, B. Dragisic, L. J. Salsberg, C. Gouliaras, M. S. Taylor, *J. Am. Chem. Soc.*, **2010**, *132*, 1646.
- [29] W. Zierkiewicz, D. Michalska, T. Zeegers-Huyskens, *Phys. Chem. Chem. Phys.*, **2010**, *12*, 13681.
- [30] P. Politzer, J. S. Murray, T. Clark, *Phys. Chem. Chem. Phys.*, **2010**, *12*, 7748.
- [31] E. Parisini, P. Metrangolo, T. Pilati, G. Resnati, G. Terraneo, *Chem. Soc. Rev.*, **2011**, *40*, 2267.
- [32] S. L. Stephens, N. R. Walker, A. C. Legon, *Phys. Chem. Chem. Phys.*, **2011**, *13*, 20736.
- [33] S. J. Grabowski, *J. Phys. Chem. A*, **2012**, *116*, 1838.
- [34] M. Erdelyi, *Chem. Soc. Rev.*, **2012**, *41*, 3547.
- [35] A. C. Legon, *Phys. Chem. Chem. Phys.*, **2010**, *12*, 7736.
- [36] G. B. Piland, P. G. Jasien, *Comput. Theor. Chem.*, **2012**, *988*, 19.

- [37] R. E. Rosenfield, R. Parthasarathy, J. D. Dunitz, *J. Am. Chem. Soc.*, **1977**, *99*, 4860.
- [38] T. N. G. Row, R. Parthasarathy, *J. Am. Chem. Soc.*, **1981**, *103*, 477.
- [39] F. T. Burling, B. M. Goldstein, *J. Am. Chem. Soc.*, **1992**, *114*, 2313.
- [40] Y. Nagao, T. Hirata, S. Goto, S. Sano, A. Kakehi, K. Iizuka, M. Shiro, *J. Am. Chem. Soc.*, **1998**, *120*, 3104.
- [41] D. B. Werz, R. Gleiter, F. Rominger, *J. Am. Chem. Soc.*, **2002**, *124*, 10638.
- [42] M. Iwaoka, S. Takemoto, S. Tomoda, *J. Am. Chem. Soc.*, **2002**, *124*, 10613.
- [43] R. Gleiter, D. B. Werz, B. J. Rausch, *Chem. Eur. J.*, **2006**, *9*, 2676.
- [44] C. Bleiholder, D. B. Werz, H. Koppel, R. Gleiter, *J. Am. Chem. Soc.*, **2006**, *128*, 2666.
- [45] M. H. Esseffar, R. Herrero, E. Quintanilla, J. Z. Dávalos, P. Jiménez, J.-L. M. Abboud, M. Yáñez, O. Mó, *Chem. Eur. J.*, **2007**, *13*, 1796.
- [46] J. S. Murray, P. Lane, P. Politzer, *J. Mol. Model.*, **2009**, *15*, 723.
- [47] F. R. Knight, A. L. Fuller, M. Bühl, A. M. Z. Slawin, J. D. Woollins, *Chem. Eur. J.*, **2010**, *16*, 7503.
- [48] L. Junming, L. Yunxiang, Y. Subin, Z. Weiliang, *Struct. Chem.*, **2011**, *22*, 757.
- [49] M. Bühl, P. Kilian, J. D. Woollins, *ChemPhysChem.*, **2011**, *12*, 2405.
- [50] G. Sánchez-Sanz, I. Alkorta, J. Elguero, *Mol. Phys.*, **2011**, *109*, 2543.
- [51] M. Jablonski, *J. Phys. Chem. A*, **2012**, *116*, 3753.
- [52] S. Scheiner, *J. Chem. Phys.*, **2011**, *134*, 094315.
- [53] S. Scheiner, *J. Phys. Chem. A*, **2011**, *115*, 11202.
- [54] S. Scheiner, *Chem. Phys. Lett.*, **2011**, *514*, 32.
- [55] Y. Gu, T. Kar, S. Scheiner, *J. Am. Chem. Soc.*, **1999**, *121*, 9411.
- [56] Y. Gu, T. Kar, S. Scheiner, *J. Mol. Struct.*, **2000**, *552*, 17.
- [57] Y. Gu, T. Kar, S. Scheiner, *J. Mol. Struct. (Theochem)*, **2000**, *500*, 441.
- [58] S. Scheiner, *Chem. Phys.*, **2011**, *387*, 79.
- [59] S. Scheiner, U. Adhikari, *J. Phys. Chem. A*, **2011**, *115*, 11101.
- [60] U. Adhikari, S. Scheiner, *J. Phys. Chem. A*, **2012**, *116*, 3487.
- [61] S. Scheiner, *J. Chem. Phys.*, **2011**, *134*, 164313.
- [62] U. Adhikari, S. Scheiner, *Chem. Phys. Lett.*, **2012**, *532*, 31.
- [63] Y. Mo, P. Bao, J. Gao, *Phys. Chem. Chem. Phys.*, **2011**, *13*, 6760.
- [64] K. Kitaura, K. Morokuma, *Int. J. Quantum Chem.*, **1976**, *10*, 325.
- [65] K. Morokuma, K. Kitaura. Energy decomposition analysis of molecular interactions. In *Chemical Applications of Atomic and Molecular Electrostatic Potentials*; Politzer, P., Truhlar, D. G., Eds.; Plenum: New York, 1981; pp 215.
- [66] K. Szalewicz, B. Jeziorski. Symmetry-adapted perturbation theory of intermolecular interactions. In *Molecular Interactions. From Van der Waals to Strongly Bound Complexes*; Scheiner, S., Ed.; Wiley: New York, 1997; pp 3.
- [67] R. Moszynski, P. E. S. Wormer, B. Jeziorski, A. van der Avoird, *J. Chem. Phys.*, **1995**, *103*, 8058.
- [68] S. F. Boys, F. Bernardi, *Mol. Phys.*, **1970**, *19*, 553.
- [69] S. Scheiner, *Comput. Theor. Chem.*, **2012**, *998*, 9-13
- [70] M. J. Frisch, J. A. Pople, J. E. Del Bene, *J. Phys. Chem.*, **1985**, *89*, 3664.
- [71] J. E. Del Bene, *J. Comput. Chem.*, **1989**, *10*, 603.
- [72] W. Wang, W. Zheng, X. Pu, N.-B. Wong, A. Tian, *J. Mol. Struct. (Theochem)*, **2003**, *625*, 25.
- [73] J. A. Altmann, M. G. Govender, T. A. Ford, *Mol. Phys.*, **2005**, *103*, 949.
- [74] C. Ganesamoorthy, M. S. Balakrishna, J. T. Mague, H. M. Tuononen, *Inorg. Chem.*, **2008**, *47*, 7035.
- [75] J. Moilanen, C. Ganesamoorthy, M. S. Balakrishna, H. M. Tuononen, *Inorg. Chem.*, **2009**, *48*, 6740.

- [76] S. Zahn, R. Frank, E. Hey-Hawkins, B. Kirchner, *Chem. Eur. J.*, **2011**, *17*, 6034.
- [77] J. E. Del Bene, I. Alkorta, G. Sanchez-Sanz, J. Elguero, *Chem. Phys. Lett.*, **2011**, *512*, 184.
- [78] J. E. Del Bene, I. Alkorta, G. Sanchez-Sanz, J. Elguero, *J. Phys. Chem. A*, **2012**, *116*, 3056.
- [79] U. Adhikari, S. Scheiner, *J. Chem. Phys.*, **2011**, *135*, 184306.
- [80] Q.-Z. Li, R. Li, X.-F. Liu, W.-Z. Li, J.-B. Cheng, *ChemPhysChem.*, **2012**, *13*, 1205.
- [81] M. Solimannejad, V. Ramezani, C. Trujillo, I. Alkorta, G. Sánchez-Sanz, J. Elguero, *J. Phys. Chem. A*, **2012**, *116*, 5199.
- [82] I. Alkorta, G. Sánchez-Sanz, J. Elguero, J. E. Del Bene, *J. Chem. Theory Comput.*, **2012**, *8*, 2320.
- [83] J. E. Del Bene, I. Alkorta, G. Sánchez-Sanz, J. Elguero, *J. Phys. Chem. A*, **2012**, *116*, 9205.
- [84] X.-L. An, R. Li, Q.-Z. Li, X.-F. Liu, W.-Z. Li, J.-B. Cheng, *J. Mol. Model.*, **2012**, *18*, 4325.
- [85] J. S. Murray, P. Lane, P. Politzer, *Int. J. Quantum Chem.*, **2007**, *107*, 2286.
- [86] P. Politzer, J. S. Murray, P. Lane, *Int. J. Quantum Chem.*, **2007**, *107*, 3046.
- [87] A. Zabardasti, A. Kakanejadifard, M. Ghasemian, M. Solimannejad, *Struct. Chem.*, **2012**, *23*, 1155.
- [88] J. E. Del Bene, I. Alkorta, G. Sanchez-Sanz, J. Elguero, *J. Phys. Chem. A*, **2011**, *115*, 13724.
- [89] V. M. Cangelosi, M. A. Pitt, W. J. Vickaryous, C. A. Allen, L. N. Zakharov, D. W. Johnson, *Cryst. Growth Des.*, **2010**, *10*, 3531.
- [90] A. Bauzá, D. Quiñonero, P. M. Deyà, A. Frontera, *Phys. Chem. Chem. Phys.*, **2012**, *14*, 14061.
- [91] G. Muller, J. Brand, S. E. Jetter, *Z. Naturforsch., B: Chem. Sci.*, **2001**, *56*, 1163.
- [92] S. B. Bushuk, F. H. Carre, D. M. H. Guy, W. E. Douglas, Y. A. Kalvinkovskya, L. G. Klapshina, A. N. Rubinov, A. P. Stupak, B. A. Bushuk, *Polyhedron*, **2004**, *23*, 2615.
- [93] S. Tschirschwitz, P. Lönnecke, E. Hey-Hawkins, *Dalton Trans.*, **2007**, *2007*, 1377.
- [94] P. Kilian, A. M. Z. Slawin, J. D. Woollins, *Chem. Eur. J.*, **2003**, *9*, 215.
- [95] M. R. Sundberg, R. Uggla, C. Viñas, F. Teixidor, S. Paavola, R. Kivekäs, *Inorg. Chem. Commun.*, **2007**, *10*, 713.
- [96] M. Widhalm, C. Kratky, *Chem. Ber.*, **1992**, *125*, 679.
- [97] A. C. Marr, M. Nieuwenhuyzen, C. L. Pollock, G. C. Saunders, *Organometallics*, **2007**, *26*, 2659.
- [98] S. Bauer, S. Tschirschwitz, P. Lönnecke, R. Frank, B. Kirchner, M. L. Clarke, E. Hey-Hawkins, *Eur. J. Inorg. Chem*, **2009**, *2009*, 2776.
- [99] P. Batail, D. Grandjean, F. Dudragne, C. Michaud, *Acta Cryst.*, **1975**, *B34*, 1367.
- [100] I. L. Dalinger, V. M. Vinogradov, S. A. Shevelev, V. S. Kuz'min, *Mendeleev Comm.*, **1996**, *6*, 13.
- [101] R. D. Chapman, R. D. Gilardi, M. F. Welker, C. B. Kreutzberger, *J. Org. Chem.*, **1999**, *64*, 960.
- [102] R. J. Butcher, R. Gilardi, K. Baum, N. J. Trivedi, *Thermochim. Acta*, **2002**, *384*, 219.
- [103] P. V. Bernhardt, G. A. Lawrance, T. W. Hambley, *Inorg. Chem.*, **1992**, *31*, 631.
- [104] C. P. Huber, Y. Ozaki, D. H. Pliura, A. C. Storer, P. R. Carey, *Biochem.*, **1982**, *21*, 3109.
- [105] E. V. Avtomonov, K. Megges, S. Wocadlo, J. Lorberth, *J. Organomet. Chem.*, **1996**, *524*, 253.
- [106] J. D. Wallis, R. J. C. Easton, J. D. Dunitz, *Helv. Chim. Acta*, **1993**, *76*, 1411.
- [107] U. Adhikari, S. Scheiner, *Chem. Phys. Lett.*, **2011**, *514*, 36.
- [108] M. Solimannejad, M. Gharabaghi, S. Scheiner, *J. Chem. Phys.*, **2011**, *134*, 024312.

Table 1. Measures of sensitivity of interaction energy to angular distortion for complexes pairing various electron acceptors with NH<sub>3</sub>. Calculations carried out at MP2/aug-cc-pVDZ level.

EA	k <sup>a</sup> kcal mol <sup>-1</sup> rad <sup>-2</sup>	BE <sup>b</sup> kcal mol <sup>-1</sup>	k/BE rad <sup>-2</sup>
pnictogen bonds			
FPH <sub>2</sub>	68.9	6.18	11.2
CIPH <sub>2</sub>	64.3	5.35	12.0
CF <sub>3</sub> PH <sub>2</sub>	25.6	3.40	7.5
chalcogen bonds			
FSH	61.1	7.92	7.7
CISH	51.2	5.44	9.4
CF <sub>3</sub> SH	9.2	3.38	2.7
halogen bonds			
FCl	70.3	10.36	6.8
ClCl	33.5	4.98	6.7
CF <sub>3</sub> Cl	9.8	2.38	4.1
H-bonds			
HOH	10.5	5.81	1.8
FOH	15.8	9.98	1.6
FH	22.3	11.63	1.9
ClH	23.0	8.27	2.8

<sup>a</sup>force constant:  $E = \frac{1}{2} k(\Delta\theta)^2$

<sup>b</sup>binding energy

Table 2. Changes in r(B-A) bond length (mÅ) caused by complexation with NH<sub>3</sub>, computed at MP2/aug-cc-pVDZ level.

B	P	S	Cl	H
CH <sub>3</sub>	0.2	-1.0	-0.7	0.4
NH <sub>2</sub>	7.0	3.9	6.1	3.9
CF <sub>3</sub>	4.2	-2.9	6.0	0.6
OH	15.2	15.4	23.7	22.9
Cl	42.8	38.6	46.9	55.2
NO <sub>2</sub>	21.9	-2.9	-60.6	198.0
F	26.5	41.0	73.4	35.0

Table 3. NBO measures of  $N_{lp} \rightarrow \sigma^*$  charge transfer energy  $E(2)$ , kcal/mol, for complexes with  $NH_3$ , computed with aug-cc-pVDZ basis set.

B	P	S	Cl	H
CH <sub>3</sub>	0.8	0.4	0.0	2.4
NH <sub>2</sub>	4.2	2.9	3.3	5.9
CF <sub>3</sub>	4.9	2.3	2.1	10.3
OH	9.2	9.0	11.5	16.0
Cl	16.5	15.8	17.6	49.1
NO <sub>2</sub>	20.1	12.2	9.1	37.9
F	18.2	28.0	51.5	42.2

Table 4. SAPT decompositions (kcal/mol) of the complexation energies of each molecule bonded to  $NH_3$ , computed with aug-cc-pVDZ basis set.

	FH <sub>2</sub> P	FHS	FCI	FH
ES	-18.2	-24.4	-35.9	-22.4
EX	22.1	31.0	51.4	21.3
IND	-19.9	-33.9	-67.2	-13.1
IND+EXIND	-4.1	-6.1	-11.1	-6.2
DISP	-6.4	-7.3	-9.0	-4.5
DISP+EXDISP	-4.9	-5.5	-6.6	-3.5

Table 5. Binding energies (kcal/mol) computed at various levels of theory for  $BH_2P \cdots NH_3$  complexes, all using the geometries optimized at the aug-cc-pVDZ level.

B	MP2		CCSD(T)
	aug-cc-pVDZ	aug-cc-pVTZ	aug-cc-pVTZ
CH <sub>3</sub>	1.33	1.58	1.53
H	1.43	1.66	1.58
NH <sub>2</sub>	2.09	2.38	2.28
CF <sub>3</sub>	3.40	3.66	3.60
OH	3.58	4.17	3.87
Cl	5.35	5.62	5.17
NO <sub>2</sub>	6.59	7.46	7.23
F	6.19	6.59	6.09

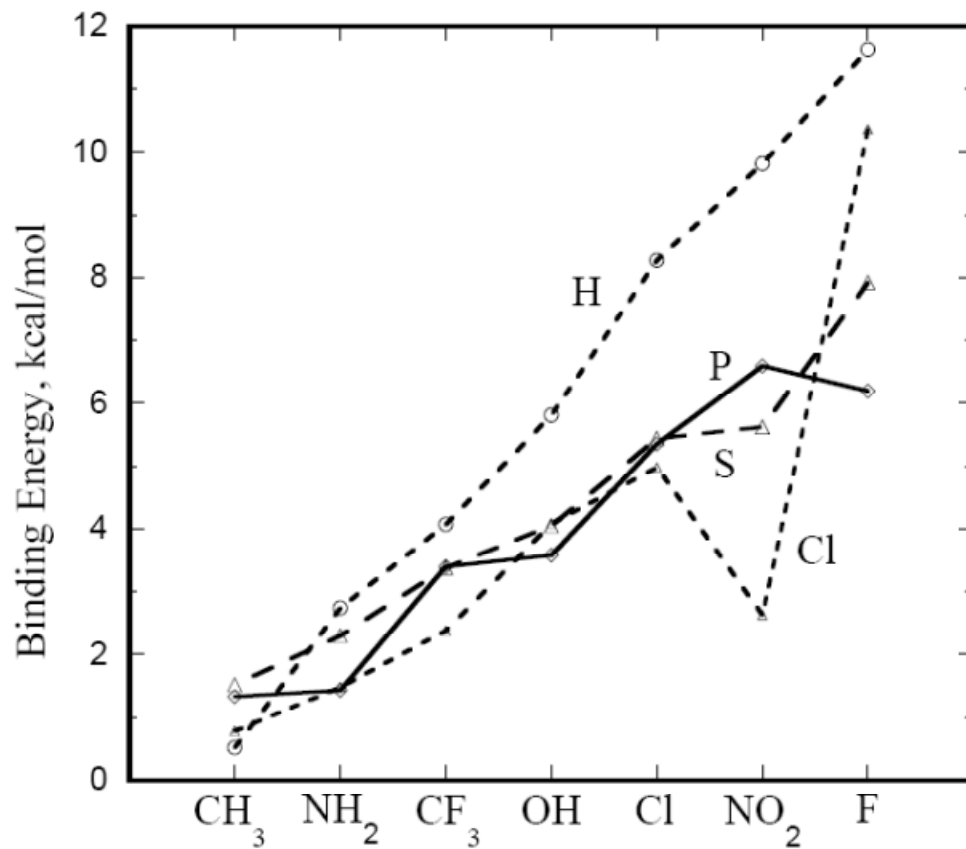


Fig 1. Binding energies of BA...NH<sub>3</sub> complexes for various B substituents, computed at MP2/aug-cc-pVDZ level with counterpoise correction. A=PH<sub>2</sub>, SH, and Cl as indicated. Values for corresponding H-bonded complexes BH...NH<sub>3</sub> are indicated by uppermost broken curve.

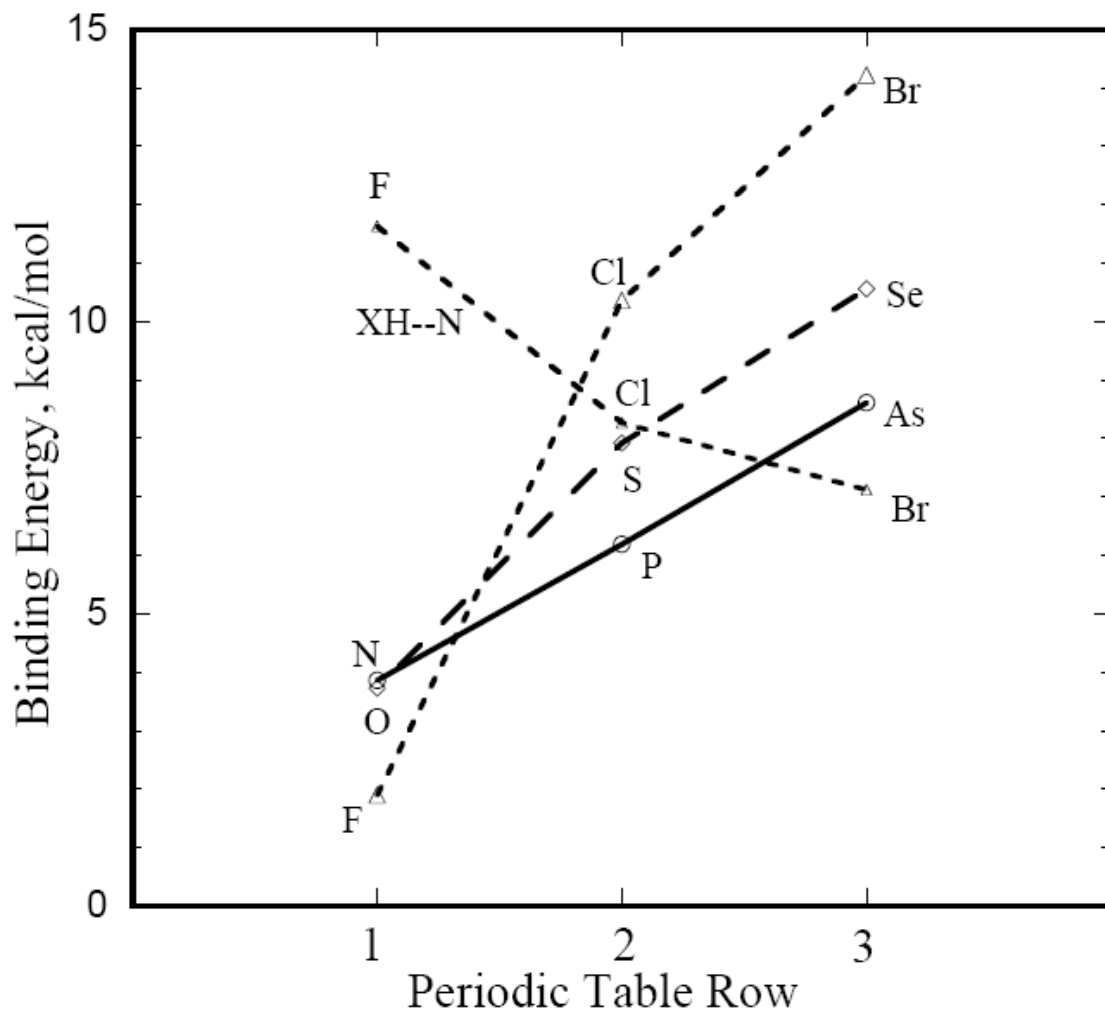


Fig 2. Binding energies of  $FA \cdots NH_3$  complexes, with  $A=PH_2$ ,  $SH$ , and  $Cl$ , and their first and third-row analogues as indicated. Also displayed are H-bond energies for  $XH$  subunits, for  $X=F$ ,  $Cl$ , and  $Br$ . All data computed at MP2/aug-cc-pVDZ level with counterpoise correction

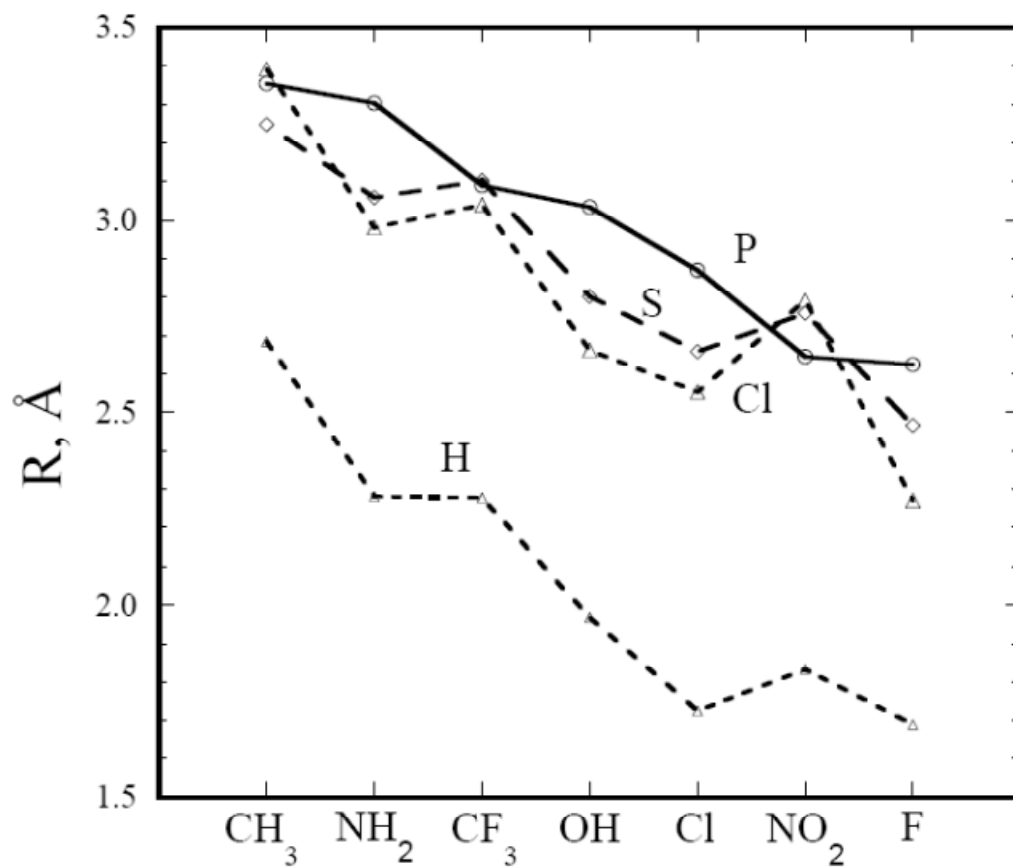


Fig 3. Intermolecular separations  $R(A\cdots N)$  of  $BA\cdots NH_3$  complexes for various B substituents.  $A=PH_2$ , SH, and Cl as indicated, computed at MP2/aug-cc-pVDZ level.  $R(H\cdots N)$  distances for corresponding H-bonded complexes  $BH\cdots NH_3$  are indicated by appropriately labeled broken curve.

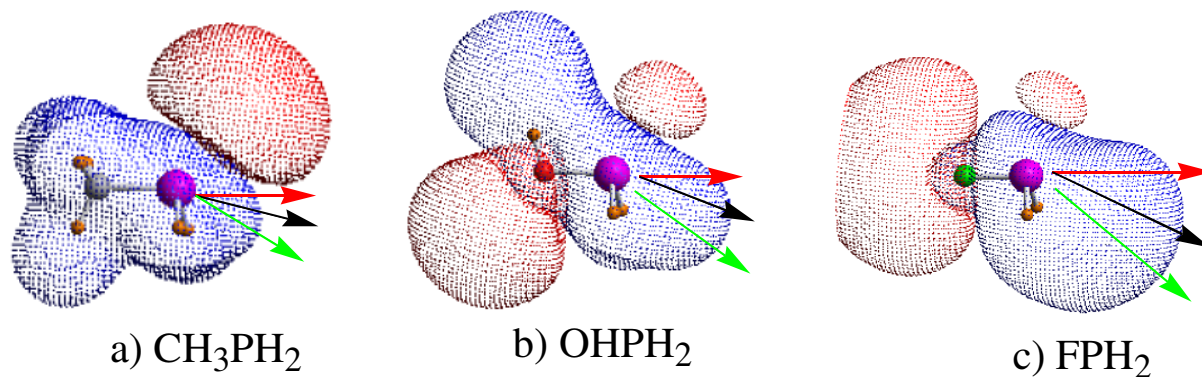


Fig 4. Electrostatic potentials of selected monomers. Positive regions are designated by blue, and negative by red, all at the  $\pm 0.01$  au contour. Red arrow indicates the B-P direction, and green arrow the direction of maximal positive electrostatic potential. The angle at which the  $\text{NH}_3$  monomer approaches within the complex is indicated by the black arrow.

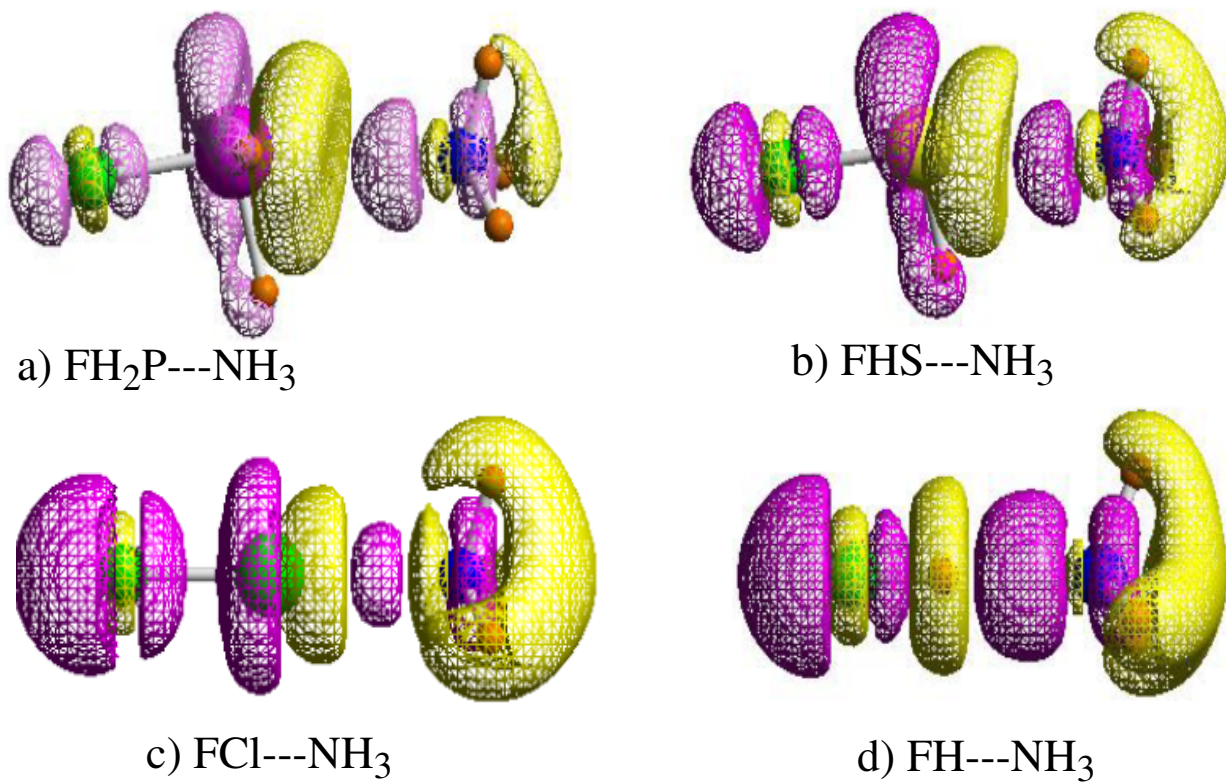


Fig 5. Redistributions of electron density that occur upon formation of each complex. Purple and yellow areas represent gains and losses of density, respectively. The contour shown corresponds to  $\pm 0.001$  au.